Macromolecular Chemistry and Physics
www.mcp-journal.de

Design and Characterization of Surface-Crosslinked Gelatin Nanoparticles for the Delivery of Hydrophilic Macromolecular Drugs

*Abdul Baseer, Aljoscha Koenneke, Josef Zapp, Saeed A. Khan, and Marc Schneider**

For nanotechnology enabled delivery of hydrophilic protein-based drugs, several polymer-based carrier systems have been used in the past to protect the sensitive load and to facilitate cellular uptake and crossing of biological barriers. This study uses gelatin, a natural and biodegradable macromolecule, as carrier material which is approved for several applications. Nanoprecipitation is used to form nanoparticles and to maintain the physicochemical integrity of gelatin, hydrophilic crosslinkers, e.g., paraformaldehyde, glutaraldehyde, carbodiimide, and transglutaminase are employed. However, these crosslinkers diffuse homogenously into the carrier matrix also crosslinking the polymeric matrix with the entrapped protein-based molecules thus rendering it inactive. Hence a hydrophobic zero-length crosslinker, diisopropylcarbodiimide, is applied to avoid diffusion into the particles. This will provide an opportunity to encapsulate protein-based drugs in the non-crosslinked matrix. The hypothesis of surface crosslinking is proven by the extent of crosslinking and more importantly by encapsulation and the release of lysozyme as a model hydrophilic protein. Furthermore, essential process parameters are evaluated such as crosslinker concentration, crosslinking time and crosslinking reaction temperature with regard to the effect on particle size, size distribution and zeta-potential of gelatin nanoparticles. The optimum formulation results in the production of gelatin nanoparticles with 200-300 nm and a polydispersity index < 0.2.

1. Introduction

The administration of macromolecular drugs such as protein- or peptide-based drugs by conventional routes suffers from certain challenges. Some of the important challenges faced by these biomolecules are their large size, hydrophilicity, short biological half-life, poor membrane permeability, phagocytic clearance, and structural instability.[1,2] They also undergo degradation in biological compartments, which leads to low bioavailability.[3] In order to circumvent these challenges, many strategies have been adopted for the delivery of hydrophilic macromolecules. Amongst which the nanotechnology-enabled delivery systems have offered great promise due to small size and sustained release properties.[4–6] In the nanoparticles-based delivery systems for peptidal drugs, the drug is entrapped, encapsulated, or attached to the nanoparticle matrix, depending upon the preparation method.[7] The submicron size of these nanoparticles is a critical parameter in the enhanced cellular uptake in contrast to micro-carrier delivery systems.[8,9] However, since these delivery systems are mostly based on hydrophobic polymers the hydrophobic environment may induce unfolding of protein-based drugs and nucleotide drugs, that consequently may result in diminished biological activity.[10–12] Moreover, the nanoparticles based on these hydrophobic biodegradable polymers have also demonstrated poor loading potential for hydrophilic drug molecules[13] and thus backbone modification was investigated.[14,15] In contrast to that, hydrophilic biopolymers which are obtained from living organisms have been found as a promising material for nanosystems to deliver hydrophilic macromolecules. This is also due to their biodegradability and excellent biocompatibility.[6,16,17] Amongst these, gelatin is one of the most versatile biomacromolecular polymers which has been predominantly used in foods,[18,19] cosmetics,[20] pharmaceuticals,[21,22] and medical applications.[23] It is a natural water soluble proteinaceous biomaterial obtained by base- or acid-catalyzed hydrolysis of collagen. Accordingly, there are two types of gelatins. Type A gelatin is produced as a result of acidic hydrolysis of collagen with an isoelectric point (IEP) between 7 and 9.[24] Type B

A. Baseer, A. Koenneke, Prof. M. Schneider
Department of Pharmacy, Biopharmaceutics and Pharmaceutical Technology
Saarland University
D-66123 Saarbrücken, Germany
E-mail: Marc.Schneider@uni-saarland.de
Dr. J. Zapp
Department of Pharmacy, Department of Pharmaceutical Biology
Saarland University
D-66123 Saarbrücken, Germany
Prof. S. A. Khan
Department of Pharmacy
Kohat University of Science and Technology
26000 Kohat, Pakistan
The ORCID identification number(s) for the author(s) of this article can be found under https://doi.org/10.1002/macp.201900260.

DOI: 10.1002/macp.201900260

gelatin is obtained by alkaline hydrolysis of collagen with IEP between 4.8 and 5.2.[25] It is an excipient mostly regarded as safe (GRAS) which is approved by the FDA for pharmaceutical applications such as plasma expanders (Gelafusal, Gelafundin) based on derivatives of gelatin.[26] It is an interesting biomaterial possessing several characteristics, for example, a) inexpensive, b) non-pyrogenic, and c) low antigenicity.[27,28] Due to its protein nature, it possesses several functionalities, such as carboxyl, amino, phenol, guanidine, and imidazole groups, which offer potential sites for conjugation or chemical modification. Due to these characteristic features, gelatin has been frequently reported in the literature as controlled release biomaterial for biologically active substances.[29] The delivery systems fabricated from gelatin include hydrogels,[30] microspheres,[31] scaffolds,[32] and nanoparticles.[33]

Hydrophilicity is one of the important physicochemical properties of gelatin due to which it is well-suited for the incorporation of hydrophilic macromolecular drugs. But, from formulation point of view, gelatin-based drug delivery systems cannot maintain their structural integrity upon exposure to aqueous environment thus disassembling and immediately releasing the incorporated payload.[34] Hence, it is important to stabilize these gelatin-based carrier systems in order to achieve physicochemical and mechanical stabilization in aqueous environment. Ever since the discovery of gelatin nanoparticles (GNPs) by Oppenheim et al.,[35] crosslinking has been an indispensable step for the preparation of stable GNPs. For this purpose, different crosslinkers have been used so far such as glutaraldehyde (GTA),[36] glyoxal,[37] genipin,[38] water soluble carbodiimide,[39] microbial transglutaminases,[40] and reduced sugars.[41] However, these crosslinkers crosslink the carrier matrix and also the loaded protein drug. The drug will not be released and might also be not active after crosslinking. Therefore, a novel strategy for the stabilization of GNPs is needed.[34]

In this study, we intend to crosslink GNPs only on the interface using hydrophobic zero-length crosslinkers in order to avoid the diffusion of crosslinker inside the nanoparticle matrix. To the best of our knowledge, the stabilization of GNPs with the application of hydrophobic zero-length crosslinkers is not reported so far. The aim of this study is to design nanosized hydrophilic gel-based particles for the delivery of hydrophilic macromolecules. The subsequent stabilization of the loaded GNPs with hydrophobic crosslinker will overcome the main drawback for flexible protein delivery. For the selective interfacial crosslinking of GNPs, we employed diisopropylcarbodiimide (DIC).

2. Results and Discussion

2.1. Preparation of DIC-Crosslinked GNPs

This research work aimed to introduce a novel formulation strategy for the physicochemical stabilization of GNPs, using the zero-length hydrophobic crosslinker, DIC. We hypothesize that the hydrophobic crosslinker due to its low polarity (hydrophobicity) might be confined in the external environment (i.e., anti-solvent phase, acetone in our case) and would not diffuse into the hydrophilic matrix of GNPs. Consequently, only the amino acid and carboxylic acid functionalities located on the colloidal interface will be coupled together thus establishing an amide crosslink on the surface of the nanoparticles. The formation of GNPs was carried out following the standard protocols of nanoprecipitation.[42] Briefly, the solvent phase (aqueous solution of gelatin) is added dropwise to the anti-solvent (acetone) containing stabilizer.[36,43] Due to diffusion of the solvent phase into the anti-solvent phase, a strong interfacial turbulence is produced which leads to precipitation of gelatin at the interface in the form of GNPs.[42,44,45] Subsequently, the crosslinker DIC was added to the nanosuspension followed by stirring for 24 h to favor crosslink formation on GNPs. The preparation procedure is shown schematically in **Figure 1**.

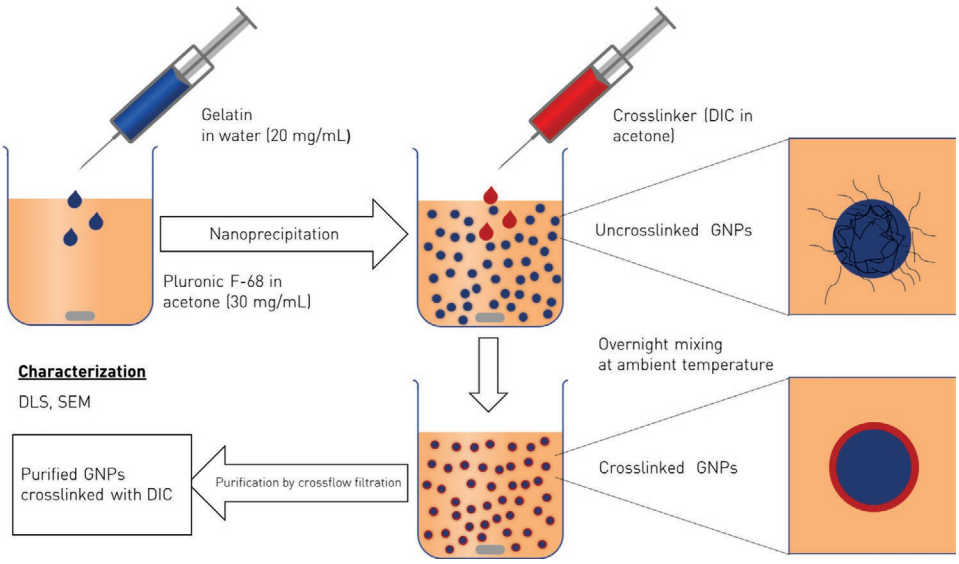

Figure 1. Schematic representation of the procedure to form GNPs via nanoprecipitation and surface crosslinking the particles by DIC.

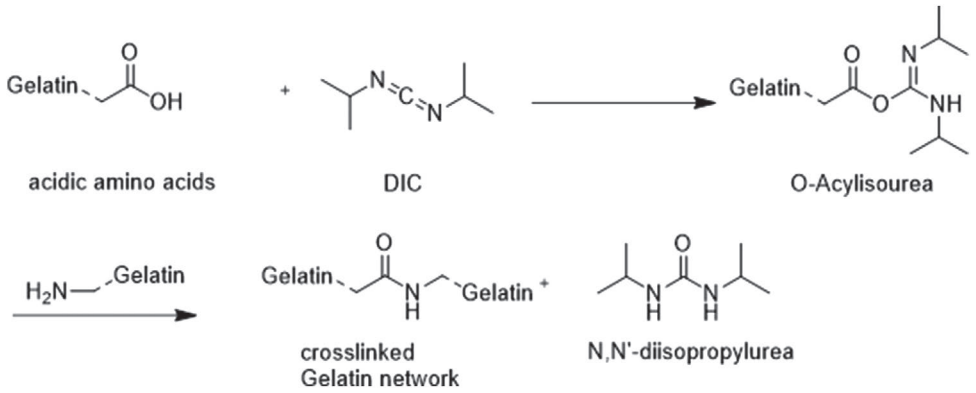

Figure 2. Schematic representation of DIC-mediated crosslinking mechanism. A) Formation of DIC-mediated activation of (–COOH) to form the unstable intermediate O-Acylisourea; and B) secondary reaction with nucleophilic substitution of free primary amino groups presented by lysine into the formerly formed DIC activated ester leading to formation of amide crosslink at GNPs interface.

2.2. Optimization of Crosslinker Concentration

Type B gelatin with bloom number 75 was used throughout the experiments which contains approximately 33×10^{-5} moles ε-amino groups per gram on the lysine and hydroxy-lysine residues, and approximately 126×10^{-5} moles carboxylic acid groups per gram on glutamic and aspartic acids.[46] The hydrophilic nature of gelatin requires the physicochemical stabilization via crosslinking. The hydrophobic crosslinker (DIC) activates the carboxylic moiety present in a peptide network forming an activated O-acylisourea which is subsequently attacked by a nucleophile present in another peptide chain, for example, primary amino groups, forming a stable amide bond which acts as intra- and inter-peptide crosslinks (**Figure 2**). The obtained GNPs when crosslinked with crosslinkers in concentration ranges from 0.99 to 3.98 mg mL^{-1} display a mean size of 250 nm with a broad size distribution [polydispersity index (PDI) > 0.2] (**Figure 3**). Monodisperse nanosuspensions were obtained for DIC concentration ≥ 4.98 mg mL^{-1} (5–15 mg mL^{-1}) revealing an optimum stability in aqueous environment. These crosslinker concentrations from 4.98 to 15 mg mL^{-1} have no influence on particle size (Figure 3).

The crosslinking was performed over 20–24 h but crosslinking time was also found to have an impact on particle stabilization. Therefore, the effect of crosslinking time on the mean size and the size distribution was studied.

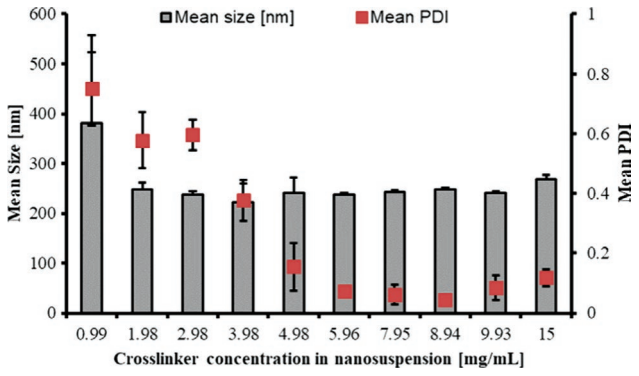

Figure 3. Effect of crosslinker concentration (DIC) on particle size and size distribution. The nanoparticles were measured in water after tenfold dilution before purification in three independent experiments ($n = 3$).

2.3. Optimum Crosslinking Time

2.3.1. Effect of DIC Concentration and Crosslinking Temperature

Using the crosslinker with two concentrations, 5 and 15 mg mL^{-1} at room temperature, resulted in optimal physicochemical stability in aqueous environment after 25–30 and 15–20 h, respectively. No agglomeration of the particles was observed. The mean sizes of crosslinked GNPs at these conditions were found to be 241.80 nm for a crosslinker concentration of 5 mg mL^{-1}, and 231.72 nm for 15 mg mL^{-1}, both formulations showed a PDI < 0.2 after 48 or 20 h, respectively. Hence, increasing the crosslinker concentration to 15 mg mL^{-1} reduced the optimum crosslinking time (**Table 1**). The whole dataset measured can be seen in Figures S1 and S2, Supporting Information.

Since the endothermic chemical reaction kinetics were increased with increase in temperature, the DIC-induced crosslinking process should also be activated. The crosslinking reaction was performed at two temperature levels, 30 °C and

Table 1. Summary of the impact of crosslinker concentration and temperature of crosslinking mixture on the optimum crosslinking time necessary for the stability of particles in aqueous environment. The mean sizes and size distribution of crosslinked nanoparticles at corresponding crosslinking time is also shown.

Crosslinker conc. [mg mL^{-1}]	Temperature [°C]	Optimum crosslinking time [h]	Mean size ± SD [nm]	Mean PDI ± SD
5	23	48	241.80 ± 30.07	0.16 ± 0.08
5	30	25	252.92 ± 16.80	0.14 ± 0.05
5	50	5	250.54 ± 11.53	0.11 ± 0.07
15	23	15	231.72 ± 4.29	0.15 ± 0.02
15	30	3	253.55 ± 9.21	0.13 ± 0.02
15	50	2	269.45 ± 9.21	0.16 ± 0.03

50 °C in an incubator using the previously used crosslinker concentrations. It was observed that the optimum crosslinking time is inversely related to temperature as expected. For a DIC concentration of 5 mg mL^{-1} the crosslinking time could be shortened to 25 h at 30 °C and 5 h at 50 °C. Consequently, for the higher crosslinker concentration the time could be shortened even further to 3 h at 30 °C and 2 h at 50 °C. Hence, it can be inferred that temperature has a direct impact on stabilization kinetics mediated by chemical crosslinking with DIC. Performing the crosslinking of GNPs suspension with DIC at higher temperatures led to a reduction in the optimum incubation time which is necessary for the physicochemical stability of GNPs in aqueous environments.

However, for all formulations, the mean particle size increased at higher temperatures. Thus, in combination with the possible encapsulation of temperature sensitive proteins, we decided to use a concentration of 15 mg mL^{-1} DIC and crosslink the particles at room temperature for 18 h to achieve a stable formulation.

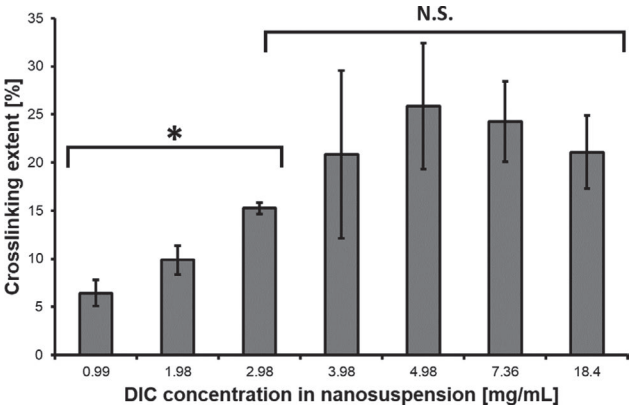

Figure 4. Relationship between % crosslinking extent and concentrations of crosslinker (DIC) in mg mL^{-1} for 18 h crosslinking time. The volumes were kept constant during the preparations. Values determined from TNBS assay by using the absorption maximum of λ_{max} = 349 nm, n = 3. N.S., statistically non-significant on the basis of $p > 0.05$ as per one-way ANOVA. *, statistically significant, $p < 0.05$ as per one-way ANOVA.

2.4. Investigation of DIC-Mediated Crosslinkability of Gelatin Nanoparticles

2.4.1. Quantification of Crosslinking Degree—TNBS Assay

The crosslinking degree of DIC-induced crosslinked GNPs was quantitatively determined by trinitro benzenesulfonic acid (TNBS) assay.[47] TNBS assay is based on spectrophotometric determination of primary amino groups in crosslinked and uncrosslinked particles. TNBS reacts with the primary amino groups under mild alkaline conditions to produce an unstable Meisenheimer complex followed by acidification which converts the unstable intermediate complex to a pale-yellow stable trinitrophenyl derivative, which can be quantified spectrophotometrically at λ_{max} = 349 nm.

Based on the absorbance of uncrosslinked and crosslinked GNPs, the total number of primary amino groups engaged in crosslinking GNPs was calculated. The result demonstrated that the crosslinking degree in GNPs after 18 h of crosslinking is proportional to the crosslinker concentration until a plateau is reached (**Figure 4**). The plateau starts from around 3.98 mg mL^{-1}. This is also supported by a statistical analysis using a one-way ANOVA analysis which states that the corresponding crosslinking degrees for DIC concentrations from 3.98 up to 18.4 mg mL^{-1} were statistically insignificant. Hence increasing the quantity of crosslinker has no influence on the percentage of the crosslinking extent within the errors of the measurement. This demonstrates a saturation of the crosslinking process. Thus, there are no more free primary amino groups which can be reached for crosslinking.

In another experiment, the crosslinking time was extended to 48 h and subsequently the crosslinking degrees were determined (**Figure 5**). According to statistical analysis (one-way ANOVA, $p > 0.05$), we see that the difference of the measured crosslinking degrees were not statistically significant. Therefore, for 48 h crosslinking the degree of crosslinking is not influenced by the concentration of crosslinker anymore. The maximum crosslinking degree found was ≈25–30%. This low amount of crosslinking might be attributed to the hydrophobic nature of the crosslinker. Due to this property of DIC, diffusion into the polar core is limited. Therefore, the uncrosslinked amino groups should be localized in the interior of nanoparticles not being exposed to the crosslinker. Consequently, a crosslinker-free core area should be obtained. This is also supported by the fact that stable nanoparticles can be prepared. If crosslinking would not be on the outside of the particles the uncrosslinked part should be dissolved not forming particulates.

Based on the results of the TNBS assay we can calculate the potential architecture assuming that all crosslinked groups are on the outside, whereas the core is not crosslinked at all. Furthermore, assuming a homogeneous distribution of the crosslinkable groups we can estimate the crosslinked versus the non-crosslinked volume resulting in a core–shell structure with an inner sphere of radius $R_{\text{uncrosslinked sphere}}$ = 111 nm and a crosslinked edge of 14 nm thickness (**Figure 6**).

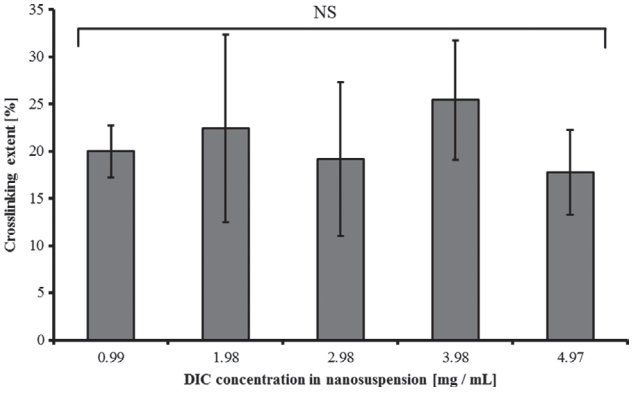

Figure 5. Relationship between % crosslinking degree and amount of crosslinker (mg mL^{-1}) for 48 h crosslinking reaction time. Values determined by TNBS assay using an absorption maximum of λ_{max} = 349 nm, n = 3. NS, statistically non-significant on the basis of $p > 0.05$ as per one-way ANOVA.

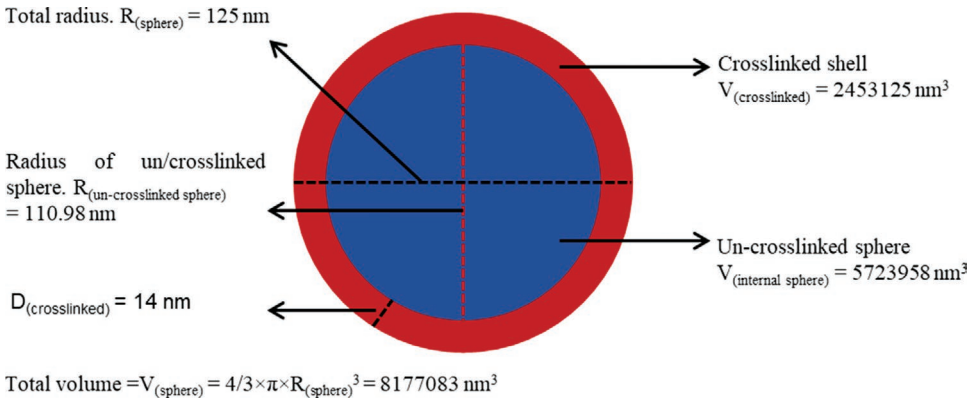

Figure 6. Estimated geometry of DIC-crosslinked GNP based on TNBS assay. $V_{(sphere)}$, total volume of GNP sphere; $V_{(internal\ sphere)}$, volume of non-crosslinked sphere; $V_{(crosslinked)}$, volume of crosslinked part of GNP; $R_{(uncrosslinked\ sphere)}$, radius of uncrosslinked part of GNP which is the interior of GNP; $R_{(sphere)}$, total radius of GNP; $D_{(crosslinked)}$, sum of the thickness of the crosslinked edge (nm).

2.4.2. Monitoring of Crosslinker after Crosslinking Reaction

Quantification of Unreacted Crosslinker—Gas Chromatography: The unreacted crosslinker (DIC) was determined quantitatively using a pre-established gas chromatography method using a flame ionization detector (GC-FID). The calibration curve was constructed after plotting concentrations of different calibration standards of DIC in acetone versus corresponding peak areas under each GC chromatogram. For this investigation of the formulations, three GNP formulations with different crosslinker amounts were considered. Afterward, these GNP colloidal dispersions were centrifuged at 20 000 × *g* for 25 min. The supernatant was extracted and analyzed for the amount of unreacted crosslinker present in each formulation of GNP suspension.

From the experimental data in **Table 2** one could conclude that the converted masses of DIC are the same for all experiments irrespective of the initial amount of crosslinker used. As the mass of gelatin and thus the number of particles and the available surface is constant within the error of the experiment, this behavior is well in line with the TNBS assay. Only a certain amount of crosslinker is being consumed in the crosslinking process of GNPs indicating that we have a saturatable process (Table 2, Figures 4 and 5). Moreover, the total amount of crosslinker utilized in the crosslinking process is extremely low. Presumably, due to hydrophobicity, the crosslinker (DIC) has only accessibility to the functional groups present at the colloidal interface of GNPs, and is not diffusing into the interior of the GNPs. Hence, when all the available reactive groups present on the interface are crosslinked, no further crosslinking takes place.

Table 2. Relationship between crosslinker amounts (mg) used initially for crosslinking and amounts of DIC consumed in crosslinking of GNPs.

Amount added initially [mg]	Unreacted amount [mg] ± SD	Reacted amount[a)] [mg] ± SD
32.4	26.36 ± 3.03	6.04 ± 3.03
48.6	44.40 ± 0.21	4.20 ± 0.21
64.8	57.38 ± 0.01	6.97 ± 0.01

[a)]The reacted amounts were found statistically insignificant on the basis of $p > 0.05$ as per one-way ANOVA.

Quantification of Diisopropylurea: A Crosslinking By-Product As elaborated above (Figure 2), DIC conjugates the carboxylate groups with the primary amino groups present in the gelatin peptide network forming an amide bond which is responsible for the physicochemical and mechanical integrity of GNPs in aqueous environment. Consequently, DIC is transformed into its corresponding by-product known as diisopropylurea (DIU) which is soluble for instance in acetone but insoluble in aqueous solutions. The DIU was quantified using ^{1}H NMR spectroscopy. The amount of DIU in the GNPs suspension was obtained after centrifuging DIC-crosslinked GNPs (24 000 × *g*, for 30 min). Afterward, the supernatant consisting of a mixture of crosslinker (DIC) and DIU dissolved in acetone was analyzed with ^{1}H NMR spectroscopy.

The proton NMR spectrum of the crosslinking mixtures showed resonances for DIU together with tiny signals for the by-product DIU providing the methyl resonances for quantification (Figure S3A, Supporting Information). In contrast to DIC the methyl protons of DIU were slightly shifted to higher field appearing almost free of superimposition in the region of the high field carbon-13 satellite of the DIC methyl resonances (Figure S3A, Supporting Information, close-up). Therefore, integration of the separate DIU methyl doublet lines as well as the DIC methyl carbon-13 satellite lines could easily be performed (Figure S3B, Supporting Information). These integration values were taken to establish the relationship between the amount of DIC and DIU, taking into account that a carbon-13 satellite resonance represented only 0.55% of the complete peak intensity. This way of quantification provided much more accurate results than a direct integration of the methyl resonances of the main compound DIC. The calculation can be seen in Equation (S1).

Looking at the ^{1}H NMR-based quantification of DIU found in the sample (**Figure 7**), it is evident that during the crosslinking process of GNPs mediated by DIC, the by-product (DIU) is formed in extremely low amounts. With a fixed mass of gelatin (20 mg), the amount of DIU formed after

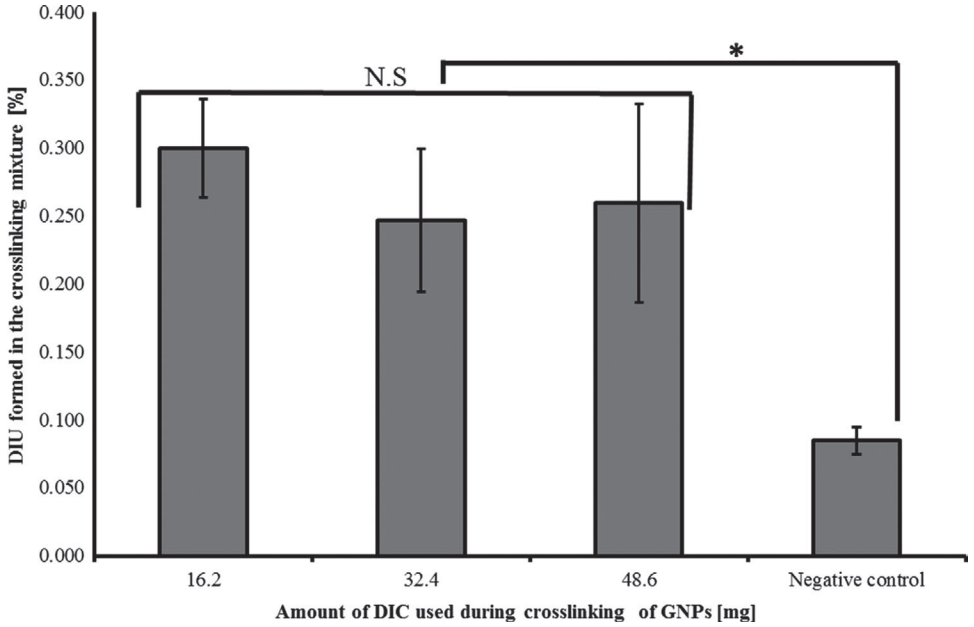

Figure 7. Quantification of the reaction by-product DIU. The diagram shows the results of the DIU quantification, calculated by the integral of the corresponding peaks for different amounts of crosslinker. Negative control: sample without gelatin. * $p < 0.05$ as per one-way ANOVA, NS, statistically non-significant.

crosslinking reaction is independent of whatever amount of DIC is being used.

Thus, from NMR and GC data, it can be also concluded that crosslinking of a certain number of available amino and carboxylic groups took place but no further crosslinking. Hence, the TNBS assay, gas chromatography, and ^{1}H NMR data support the surface-restricted crosslinking behavior of hydrophobic crosslinker DIC and the simple core–shell model derived.

2.5. Zeta Potential of DIC-Crosslinked GNPs

The zeta potential of DIC-crosslinked GNPs purified via tangential flow filtration (TFF) was measured at different pH values. Since gelatin is a polyamphoteric biopolymer possessing both anionic and cationic functional groups, the overall charge of gelatin backbone is dependent on the pH of the surrounding. Since type B gelatin possesses relatively high proportion of acidic amino groups like aspartate and glutamate as compared to basic amino groups (e.g., lysine, hydroxy-lysine, arginine) low IEP (4–5) is the consequence.

It is evident from the zeta potential profile (**Figure 8**) that the GNPs possess slightly positive zeta potential (between +11 and +7 mV) at pH 5 and 6, respectively. For pH larger than 7, the zeta potential is shifting to negative values. At neutral pH 7, the zeta potential is almost zero. The zeta potential of GNPs suspension is expected to be zero at the isoelectric pH of type B gelatin (pH 4.7–5.4). However, a shift of the IEP of gelatin toward 6–7 (Figure 8) is observed. This phenomenon can be associated to the DIC crosslinking and its crosslinking mechanism. Gelatin contains twice as much arginine (5%) than L-lysine (2.7%).[48,49] Assuming that all lysine residues are engaged in crosslinking leaves free arginin which is not involved in crosslinking. The pKa value of arginine is found to be 12.1 leading to a shift to higher pH values.[50] In consequence to this shift of IEP to higher pH values, the zeta potential of DIC-crosslinked GNPs is close to neutral for neutral pH.

2.6. Morphological Characterization–Scanning Electron Microscopy

The scanning electron microscopy (SEM) analysis of DIC-crosslinked GNPs revealed that the nanoparticles have spherical morphology (**Figure 9**). The mean size calculated from SEM image using imageJ is summarized in **Table 3**. As can

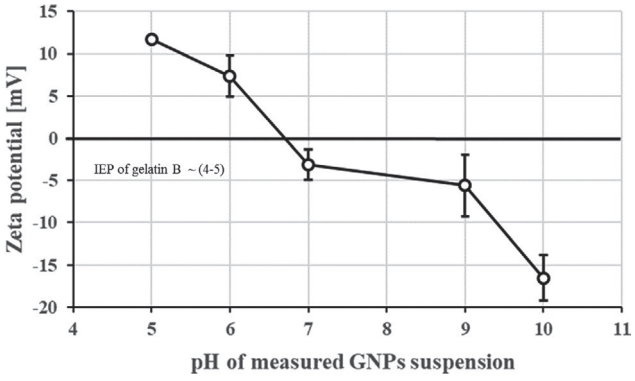

Figure 8. Zeta potential of type B GNPs crosslinked with DIC 15 mg mL^{-1} measured at different pH values after TFF-based purification.

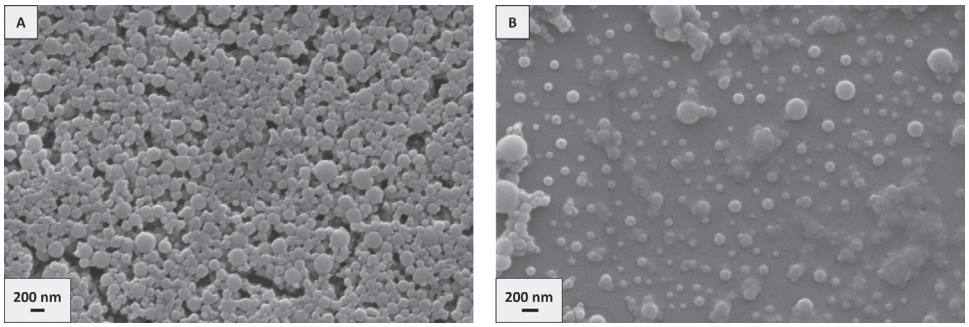

Figure 9. SEM micrographs of DIC-crosslinked GNPs purified via ultra-filtration using tangential flow filtration performed with a regenerated cellulose membrane of 100 kDa pore size. A) Concentrated sample. B) Diluted sample.

Table 3. Size characterization of DIC-crosslinked GNPs purified via tangential flow filtration (TFF).

Formulation	Purification method	Size ± SD [nm]	
		DLS[a)]	SEM[b)]
DIC-crosslinked GNPs	TFF filtration (RC[c] membrane of 100 kDa)	224.5 ± 1.87 (0.12)	145.33 ± 58.12

[a)]Term in parenthesis represent PDI; [b)]100 particles analyzed using imageJ software. RC[c], regenerated cellulose.

be seen, the mean size of GNPs determined by SEM micrograph is lower than that of DLS analysis. Presumably, this is due to drying of samples before SEM imaging in contrast to the hydrated particles in aqueous dispersion.[42,51]

2.7. Drug Loading and Release

Lysozyme in different mass ratios of drug to polymer was added to the gelatin solution used for GNPs preparation. Afterward the GNPs were subsequently crosslinked with DIC for 48 h (the optimum crosslinking time for lysozyme-loaded GNPs). The drug to polymer mass ratios included 2.5%, 5%, 10%, 25%, and 50%. The mean size of loaded GNPs (**Table 4**) did not change compared to the unloaded GNPs within the range of 2.5–5% ratio of lysozyme to gelatin (i.e., 170–190 nm). For higher amounts of loaded lysozyme (loading ratio of 5–25%) the size increased by 20–30 nm. However, all particle formulations showed a narrow size distribution (Table 4). Loading lysozyme above 25% led to visible aggregate formation hence unstable nanosuspensions. Thus, the maximum loading ratio of lysozyme to gelatin was found to be 25%.

The zeta potential values of lysozyme-loaded GNPs was observed to be highly positive at neutral pH as compared to unloaded GNPs possessing slightly negative zeta potential at neutral pH (Table 4). The positive zeta potential of lysozyme-loaded GNPs could be attributed to the successful loading of the lysozyme molecules which are positively charged at these conditions.

The entrapment efficiency is above 80% for all amounts of lysozyme leading to stable nanosuspensions. The loading is constantly increasing and can be adjusted up to 12%. The in vitro release profile of lysozyme loaded GNPs from the gelatin matrix, demonstrated that about 40% of lysozyme was released in the initial 0.5 h (**Figure 10**). This fast burst release has also been reported by other investigators.[52] The burst release of approximately 40–50% was followed by a sustained release up to an extent of 90–100% for 24 h. Lysozyme is a cationic polypeptide composed of 129 amino acids containing many basic as well as acidic amino acid residues[53] thus providing a favorable environment for crosslinking reaction by crosslinker (e.g., DIC). Nevertheless, the maximum release up to 90–100% of lysozyme from DIC-mediated crosslinked GNPs matrix reveals that the crosslinker is only slightly involved in crosslinking the payload allowing high fraction of release. In contrast, the

Table 4. Physicochemical properties of unloaded and lysozyme-loaded GNPs. DLS measurements were performed in acetone.

Used lysozyme [% m/m of gelatin]	Size ± SD [nm]	PDI ± SD	Zeta potential at pH 7 [mV]	Entrapment efficiency ± SD [%]	Loading efficiency ± SD [%]
Unloaded GNPs	184.19 ± 5.20	0.09 ± 0.05	−4.43 ± 2.30	—	—
2.5	178.84 ± 10.26	0.07 ± 0.01	10.66 ± 2.30	99.60 ± 3.35	3.35 ± 1.33
5	184.76 ± 7.20	0.08 ± 0.02	10.57 ± 0.76	87.01 ± 4.79	4.79 ± 1.16
10	205.00 ± 10.00	0.09 ± 0.02	28.14 ± 0.97	93.97 ± 9.87	9.87 ± 1.71
25	221.25 ± 7.00	0.07 ± 0.02	—	80.92 ± 12.20	12.20 ± 5.11
30	ND	ND	ND	ND	ND
40	ND	ND	ND	ND	ND
50	ND	ND	ND	ND	ND

ND, not determined due to visible precipitate formation.

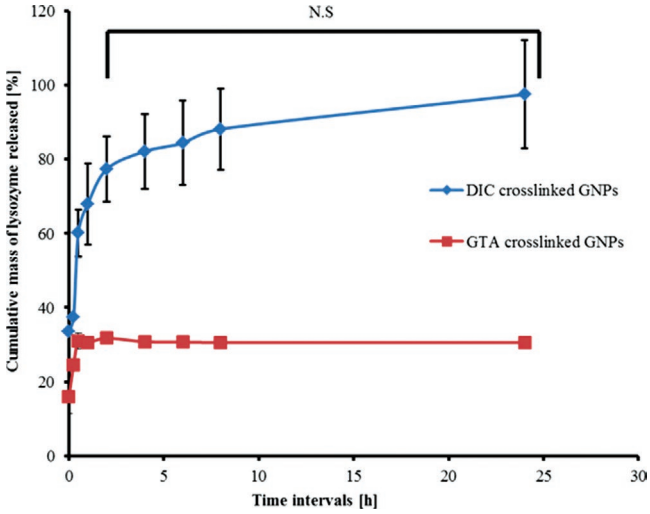

Figure 10. In vitro release profile of DIC- and GTA-crosslinked gelatin nanoparticles loaded with lysozyme in phosphate buffer saline (PBS) pH 7.4 as release medium at 37 °C. N.S., non-significant statistically on the basis of $p > 0.05$ using one-way ANOVA.

release from the standard GNP stabilized by GTA crosslinking showed a maximum of only 30% release of lysozyme while 70% is not available for release. As GTA is a hydrophilic homobifunctional crosslinker which also diffused into the core of the nano-particulate matrix also crosslinking the drug load.

2.8. Determination of Biological Activity

To determine the biological activity of lysozyme after particle crosslinking either with DIC, or with GTA, a *Micrococcus lysodeikticus* assay was used. The particles were incubated with the gem for 24 h and the activity was measured as described. DIC-GNPs were crosslinked for 48 h, as described before. The crosslinking time for GTA-GNPs was reduced from 48 to 24 h, as under this condition stable particles could be prepared and, due to the lower crosslinking degree, more protein might be uncrosslinked and active.

The activity-based determined amounts of lysozyme, that is, turbidimetric bioassay, were compared with HPLC-based determined amounts. The released samples from crosslinked GNPs in PBS (pH 7.4) following incubation for 24 h at 37 °C with continuous shaking at 400 rpm were analyzed using both assays simultaneously. The results are depicted for both types of GNP systems in **Table 5**.

The analysis of the released amount clearly indicates that more lysozyme can be released from the DIC-crosslinked system compared to the GTA-crosslinked system as already seen in Section 2.7. Looking at the turbidimetric assay it is evident that during the formation of loaded GNPs and subsequently crosslinking with DIC, the biological activity of encapsulated lysozyme is preserved. For both types of particles, only a small fraction of 11% is released and seems not to be active anymore (difference between the released amount and the active amount). Notably, the enzymatic activity of lysozyme released from GTA-crosslinked GNPs is clearly lower than the activity of the amount released from the surface-crosslinked DIC particles.

Table 5. Comparison between lysozyme amounts analyzed via turbidimetric assay and HPLC assay.

Sampling time [h]	GTA-GNPs[a)]		DIC-GNPs[b)]	
	Activity [%]	Release [%]	Activity [%]	Release [%]
24	36.67 ± 4.26	48.11 ± 2.83	84.42 ± 8.18	95.15 ± 7.15

The data is an average of three independent experiments ($n = 3$); [a)]Crosslinking time: 24 h; [b)]Crosslinking time: 48 h.

The lower activity and correspondingly the low released extent of lysozyme in the case of GTA-crosslinked GNPs can be attributed to inter-molecular crosslinking (gelatin–lysozyme). In contrast, the higher activity and correspondingly, the higher release extent of lysozyme from DIC-crosslinked GNPs matrices is a clear indication that the hydrophobic crosslinker (DIC) is involved to a lower extent in the inter-molecular conjugation between lysozyme and the carrier molecule (gelatin). After comparing the release data of GTA-GNPs crosslinked for 24 h with the release data of GTA-GNPs crosslinked for 48 h (see Figure 10), it is evident that the release extent of lysozyme is higher than the release shown in Figure 10 due to shorter crosslinking time. But, it is also notable that although the release is high, the related activity is much lower. This supports our hypothesis as for longer crosslinking, the release and the corresponding activity would be even lower.

Therefore, it can be inferred that the intended therapeutic activity of encapsulated peptide-based cargo is not interfered following crosslinking with hydrophobic zero-length crosslinker, that is, DIC.

3. Experimental Section

3.1. Materials

Gelatin type B Bloom 75 from bovine skin, pluronic F-68 (Poloxamer 188) and DIC (reagent grade) were purchased from Sigma-Aldrich (Steinheim, Germany). Hen-egg-white lysozyme and GTA aqueous solution (25% w/w, grade II) was purchased from Sigma-Aldrich, Steinheim, Germany. The lyophilized powder consisting of *M. lysodeikticus* ATCC 4698 cells as a substrate for lysozyme was purchased from Sigma-Aldrich, Steinheim, Germany. Acetone was obtained from Fischer Chemicals Ltd., (Loughborough, UK). Milli-Q water with a resistivity of 18.2 MΩ $cm^{-1}$was used throughout the experiments. TFF cassettes fitted with modified regenerated cellulose material (Hydrosart) with an MWCO of 100 kDa was purchased from Sartorius Stedim Biotech Ltd. (Göttingen, Germany).

3.2. Nanoparticle Fabrication by Nanoprecipitation

GNPs were fabricated using the established formulation recipe based on the nanoprecipitation technique.[42] Briefly, the solvent

phase was prepared by dissolving 20 mg of gelatin in 1 mL of deionized water at 50 °C. Afterward, the solvent phase was added dropwise to the anti-solvent phase consisting of acetone containing Poloxamer 188 (3% w/v). Subsequently, the GNPs were crosslinked with varying amounts of DIC solution in acetone from its stock solution (69.16% w/v) for varying crosslinking time intervals. Finally, the crude nanosuspension was purified using ultra-filtration in TFF mode to remove the unreacted crosslinker (DIC), its by-products and excess amounts of stabilizers (Poloxamer 188). Nanoparticles were washed using TFF before morphological characterization. To measure the colloidal properties during the optimization process, GNPs without purification were analyzed by dynamic light scattering (DLS).

3.2.1. Formulation Optimization

In order to demonstrate an optimum stability in aqueous environment, the GNPs should be sufficiently crosslinked. In this connection, various parameters such as crosslinker concentration, crosslinking time (incubation time), and crosslinking reaction temperature were investigated for their influence on particle size, size distribution, and zeta potential.

Influence of the Crosslinker Concentration: The crude suspension of GNPs was allowed to react with varying concentrations of DIC (0.99–15 mg mL^{-1}) to investigate its possible impact on mean particle size and size distribution. The gelatin concentration in the solvent phase was 20 mg mL^{-1}, the solvent/non-solvent ratio was 1:15, and the stabilizer concentration was 3% w/v.

Influence of the Crosslinking Time: In order to investigate the minimum crosslinking reaction time, the nanosuspension was allowed to react with the crosslinker at different crosslinking incubation times (0.5–48 h). The gelatin concentration in the solvent phase was kept constant (20 mg mL^{-1}), the Poloxamer concentration in the non-solvent (acetone) was also kept constant at 3% w/v. The crosslinking incubation time was studied for two concentrations of DIC, 5 and 15 mg mL^{-1}.

Temperature of the Crosslinking Mixture: In addition, the nanosuspension was also allowed to react with the crosslinker at different temperatures: room temperature, 30 °C, and 50 °C. The influence of reaction temperature was evaluated by investigating the physicochemical attributes of the crosslinked GNPs.

3.3. Loading of Gelatin Nanoparticles with Model Protein Drug

As a proof of concept that a crosslinkable hydrophilic macromolecule can be incorporated and released, lysozyme was employed. The molecular structure of lysozyme possesses both primary amino groups as well as non-bonded carboxylic groups,[54] so maximum probability for chemical crosslinking caused by any crosslinker including DIC was given.

The GNPs were loaded with lysozyme following matrix incorporation methodology.[55] Briefly, 20 mg of gelatin were dissolved in water at 50 °C. Subsequently, lysozyme in different amounts was added to the gelatin solution. Afterward, the solvent phase containing gelatin and the payload were added to the anti-solvent phase (15 mL acetone containing Poloxamer 188). Subsequently, the nanosuspension was crosslinked with 347 µL DIC solution (taken from 69.16% w/v stock solution of DIC in acetone) and stirred for 20–24 h. Crosslinked GNPs were purified using TFF (Vivaflow 50 R, Sartorius Stedim Biotech Ltd., Göttingen, Germany) using an ultra-filtration membrane composed of modified regenerated cellulose with a pore size of 100 kDa. After purification, the loaded GNPs were characterized for mean size (*z*-average), size distribution, and zeta potential.

3.4. Nanoparticle Characterization

3.4.1. Determination of Size and Surface Charge

The particle size and size distribution of DIC-crosslinked GNPs was measured after overnight crosslinking before and after purification. The size (*z*-average mean), size distribution, and zeta potential were measured in triplicates for each batch by DLS using the Zetasizer nano-ZS (Malvern instruments, Ltd., Malvern, UK). All samples were diluted tenfold in Milli-Q water before measurements. Formulations with a PDI below 0.2 were assumed to be acceptable with respect to the size distribution.

3.4.2. Nanoparticle Morphology by Scanning Electron Microscopy

For SEM sample preparation, a silicon wafer was mounted on a metal hub using carbon adhesive tape. Then a drop of TFF-purified nanosuspension was placed onto the silicon wafer. Subsequently, samples were dried by overnight evaporation under ambient conditions. Samples were then coated with a gold layer of ≈15 nm using sputter coater Q150 RES, (Quorum Technologies Ltd, East Grinstead, UK). SEM images were then obtained by SEM (EVO HD15 Carl Zeiss Microscopy GmbH, Jena, Germany).

3.5. Determination of Crosslinking Extent

For quantitative determination of percentage crosslinking degree of DIC-crosslinked GNPs, an established trinitro-benzene sulfonic (TNBS) assay was employed.[47] Briefly, 10–12 mg lyophilized GNPs (both crosslinked and uncrosslinked) were dispersed in 1 mL of 4% sodium bicarbonate ($NaHCO_3$) and 1 mL of 0.5% TNBS. The mixture was then kept at 40 °C for 4 h. Then, 3 mL of 6 N HCl was added and the mixture was autoclaved at 120 °C and 1.03–1.17 bar for 1 h.[47] The hydrolysate was diluted to 10 mL with deionized water and extracted with ethyl acetate to remove the unreacted TNBS. A 5 mL aliquot of the aqueous phase was diluted to 25 mL with water and the absorbance was recorded at λ_{max} = 349 nm using a Perkin-Elmer Lambda35 UV-vis spectrophotometer (Rodgau, Germany) against a blank.

The blanks were prepared following the same procedure without addition of gelatin. The number of primary amino

groups was utilized as measure for crosslinking extent using Equation (1)

$$\frac{\text{Moles of primary amino groups}}{\text{Mass of gelatin in gram}} = \frac{2(\text{Absorbance})(0.025\text{L})}{(1.46\times10^4\,\text{L mole}^{-1}\,\text{cm}^{-1})(b)(x)} \quad (1)$$

where 1.46×10^4 L mole^{-1} cm^{-1} is the molar absorptivity of TNB-lys, b is the path length in centimeters, and x is the sample weight in grams.

3.6. Quantification of Unreacted Crosslinker (DIC)

Gas chromatograms of unreacted crosslinker (DIC) in acetone were recorded with a gas chromatograph (GC) (Shimadzu GC-2010, Japan) coupled with a flame ionization detector (FID) (Shimadzu GC-2010, Japan). The analytical method proposed by Sigma-Aldrich was re-validated after necessary modifications. The supernatant was isolated by centrifugation of DIC-crosslinked GNPs at 24 000 × g for 20 min. Subsequently, the supernatant was analyzed for unreacted DIC left in the nanosuspension using the validated method of gas chromatography.

3.7. Quantification of Crosslinking By-Product (Diisopropylurea)

The crosslinker DIC was after crosslinking of GNPs converted to its by-product DIU. Hence for the quantitative determination of DIU, ^{1}H NMR spectra were recorded at 298 K in acetone-d_6 with a Bruker Avance 500 spectrometer (Bruker, BioSpin GmbH, Rheinstetten, Germany) equipped with a 5 mm BBO probe. The chemical shifts were reported in parts per million (ppm) relative to the solvent peak at δ_H 2.05. All ^{1}H NMR spectra must be recorded with a sufficient number of scans, typically NS = 128, to give an acceptable S/N, because the peaks of interest, the DIU methyl protons, were in the same range as those achieved for the carbon-13 satellites of the DIC methyl groups.

which can be determined by employing an already established method based on reversed-phase HPLC in gradient elution mode[56] with slight modifications. In brief, an Ultimate 3000 series HPLC system, Rapid Speed (Thermo Fisher Scientific, Waltham, MA, USA) equipped with a quaternary pump and a Dionex Ultimate 3000 UV-vis detector with a LiChrospher 100 RP-18e column (5 µm material, 4 × 125 mm, Merck KGaA, Darmstadt, Germany) was used. The column oven was heated up to 25 °C. The mobile phase consisted of two mobile phases, that is, mobile phase A (90% water and 10% acetonitrile acidified with 0.1% v/v trifluoroacetic acid) and B (90% acetonitrile and 10% Milli-Q water acidified with 0.1% v/v trifluoroacetic acid). The gradient started with 100% mobile phase A and decreased linearly up to 100% mobile phase B in 15 min. Afterwards, from 15 to 20 min, the column was equilibrated with 100% mobile phase A. The flow rate of mobile phase was adjusted to 0.8 mL min^{-1}. For the detection and quantification of lysozyme, the detector was set to 220 nm. The injection volume of the sample was 20 µL. For data analysis, the chromatography software Chromeleon 6.8 Chromatography Data System (Thermo Fisher Scientific, Waltham, MA, USA) was used, and the quantification was based on peak integration with the help of software thus recording the area under the chromatographic peak appearing at a retention time of 8.9 min.

The lysozyme-loaded GNPs (both crosslinked and uncrosslinked) were subjected to washing with three times centrifugation (20 000 × g for 20 min) followed by re-dispersing in acetone (a non-solvent for lysozyme) after each centrifugation. The purified pellet of lysozyme-loaded GNPs was isolated. For the determination of encapsulation efficiency (EE%), 5 mg of uncrosslinked lysozyme-loaded nanoparticles were dissolved in 5 mL phosphate buffer saline (PBS) at pH 7.4 at room temperature (23 ± 2 °C). After dissolution of the nanoparticles, the samples were measured using gradient elution HPLC. A calibration curve was constructed with different concentrations of lysozyme in PBS at pH 7.4. The entrapment efficiency (EE%) was determined using Equation (2)

$$\text{Entrapment efficiency (\%)} = \frac{\text{Weight of drug in nanoparticles/Weight of nanoparticles}}{\text{Weight of durg used/Weight of gelatin used}} \times 100 \quad (2)$$

3.8. Measurement of Drug Content and In Vitro Release

The model hydrophilic protein, that is, lysozyme was loaded into DIC-crosslinked GNPs in different drug/polymer ratios. The ratios ranged from 2.5% to 50%. The lysozyme was loaded in GNPs by adding the drug substance into the gelatin matrix solution prior to nanoparticles formation via nanoprecipitation. After particle formation they were stabilized by crosslinking with DIC. The loaded nanoparticles were physicochemically characterized including size, size distribution, and zeta potential. The lysozyme content in nanoparticles was evaluated in terms of entrapment efficiency (EE%),

For the determination of the in vitro release profile, a known amount of lysozyme-loaded GNPs after purification with acetone was dispersed in PBS (pH 7.4) maintained at (37 ± 0.5) °C. The release medium was stirred at 400 rpm using a mechanical shaker. At pre-determined time points, 1 mL supernatant was withdrawn and centrifuged at 20 000 × g for 20 min. The withdrawn aliquots were replaced with fresh release medium to maintain sink conditions. The pellets were re-dispersed and added to the original dissolution medium, keeping the particles concentration constant. The aliquots withdrawn from the supernatant were analyzed using RP-HPLC in order to quantify the fraction of lysozyme released at a particular time

point. Afterwards, the percentage cumulative mass of lysozyme released from crosslinked GNPs at its corresponding time points was calculated.

3.9. Determination of Biological Activity

This assay was based on the hydrolytic activity of lysozyme on its substrate *M. lysodeikticus*, a gram positive bacterium. For this assay, lyophilized crosslinked lysozyme-loaded GNPs (8 mg) were dispersed in 4 mL PBS (pH 7.4). After 24 h incubation at 37 °C, 0.1 mL supernatant was withdrawn from the release medium and analyzed using the turbidimetric assay. For comparison, the release from GTA-crosslinked GNPs loaded with lysozyme was also measured. The quantification of enzymatic activity of lysozyme released from DIC-crosslinked GNPs was performed using standard protocols as provided by the supplier (Sigma-Aldrich). In brief, the substrate suspension (0.015% w/v) was prepared after dissolving lyophilized cells of *M. lysodeikticus* in PBS at pH 7.4. Then 2.5 mL of the substrate suspension was added to a suitable cuvette of 1 cm path length. Afterwards, 0.1 mL sample from the supernatant of lysozyme-loaded GNPs was added to the substrate suspension and carefully mixed. The decrease in absorption was recorded at 450 nm ($\Delta A_{450\ nm}$) after 1 min using UV-vis spectrophotometer at 25 °C. For quantification, known concentrations of lysozyme were treated in the same way as described for the lysozyme-loaded GNPs to obtain a calibration curve (ΔA_{450nm} per minute against known concentrations of lysozyme [μg/mL]). From this the masses of lysozyme could be determined which were then normalized to the highest activity for easier comparison.

4. Conclusion

This research work demonstrates a unique and novel approach of stabilization of GNPs with the aid of selective surface crosslinking of the colloidal interface of GNPs. This was achieved by applying a hydrophobic zero-length crosslinker, that is, DIC. Crosslinking of GNPs produced, as a result of nanoprecipitation, GNPs with sizes of 200–300 nm. The surface of DIC-crosslinked GNPs is positively charged at pH close to IEPs of gelatin. This shift in IEP is possibly due to the predominantly present protonated primary amino groups which are still uncrosslinked. The crosslinking degree was increased proportionally with increasing crosslinker concentration until an equilibrium crosslinking degree was achieved (approximately 25–30%) which was not affected by increasing the crosslinker concentration and crosslinking time. The morphology of so-designed GNPs indicates spherical geometry as confirmed by SEM analysis. There is a negligible crosslinking between gelatin matrix and lysozyme as evident from 90–100% release of lysozyme in the release medium. The activity of encapsulated lysozyme is mainly conserved after encapsulation which is in contrast to the crosslinking with GTA. In addition, the GTA-crosslinked GNPs loaded with lysozyme show only 30% release of lysozyme while a significant fraction around 70% is believed to be covalently attached with the gelatin matrix. The surface-specific crosslinking can be inferred from the large released amount of lysozyme but also from the consumed amount of crosslinker showing a saturatable process. Therefore, it can be concluded that this surface crosslinked gelatin-based nano-delivery system presents an excellent opportunity for the delivery of lysozyme as a model drug for hydrophilic macromolecules such as peptide-based bioactive compounds.

Supporting Information

Supporting Information is available from the Wiley Online Library or from the author.

Acknowledgements

This work was supported by Higher Education Commission of Pakistan (No. PD/OS-II/Batch-5/Germany 2014/38852) and the German Academic Exchange Service (No. A/13/91549598).

Conflict of Interest

The authors declare no conflict of interest.

Keywords

diisopropylcarbodiimide, hydrophilic macromolecular drugs, interfacial crosslinking, nanoprecipitation, zero-length hydrophobic crosslinkers

Received: June 18, 2019
Revised: July 29, 2019
Published online: August 23, 2019

[1] L. R. Brown, *Expert Opin. Drug Delivery* **2005**, *2*, 29.
[2] V. Agrahari, A. K. Mitra, *Ther. Delivery* **2016**, *7*, 257.
[3] A. Aubree-Lecat, M. C. Duban, S. Demignot, M. Domurado, P. Fournie, D. Domurado, *J. Pharmacokinet. Biopharm.* **1993**, *21*, 75.
[4] F. Qian, F. Cui, J. Ding, C. Tang, C. Yin, *Biomacromolecules* **2006**, *7*, 2722.
[5] T. R. Kumar, K. Soppimath, S. K. Nachaegari, *Curr. Pharm. Biotechnol.* **2006**, *7*, 261.
[6] K. Janes, P. Calvo, M. Alonso, *Adv. Drug Delivery Rev.* **2001**, *47*, 83.
[7] M. Hamidi, A. Azadi, P. Rafiei, *Adv. Drug Delivery Rev.* **2008**, *60*, 1638.
[8] J. Davda, V. Labhasetwar, *Int. J. Pharm.* **2002**, *233*, 51.
[9] L. Treuel, X. Jiang, G. U. Nienhaus, *J. R. Soc., Interface* **2013**, *10*, 20120939.
[10] C. P. Reis, R. J. Neufeld, A. J. Ribeiro, F. Veiga, *Nanomedicine* **2006**, *2*, 8.
[11] T. Govender, S. Stolnik, M. C. Garnett, L. Illum, S. S. Davis, *J. Controlled Release* **1999**, *57*, 171.
[12] U. Bilati, E. Allémann, E. Doelker, *Eur. J. Pharm. Sci.* **2005**, *24*, 67.
[13] T. S. J. Kashi, S. Eskandarion, M. Esfandyari-Manesh, S. M. A. Marashi, N. Samadi, S. M. Fatemi, F. Atyabi, S. Eshraghi, R. Dinarvand, *Int. J. Nanomed.* **2012**, *7*, 221.
[14] R. Rietscher, J. A. Czaplewska, T. C. Majdanski, M. Gottschaldt, U. S. Schubert, M. Schneider, C.-M. Lehr, *Int. J. Pharm.* **2016**, *500*, 187.

[15] R. Rietscher, M. Schröder, J. Janke, J. Czaplewska, M. Gottschaldt, R. Scherließ, A. Hanefeld, U. S. Schubert, M. Schneider, P. A. Knolle, *Eur. J. Pharm. Biopharm.* **2016**, *102*, 20.
[16] Y. Xu, Y. Du, *Int. J. Pharm.* **2003**, *250*, 215.
[17] A. Vila, A. Sanchez, K. Janes, I. Behrens, T. Kissel, J. L. Vila Jato, M. J. Alonso, *Eur. J. Pharm. Biopharm.* **2004**, *57*, 123.
[18] Z. N. Hanani, Y. Roos, J. Kerry, *Int. J. Biol. Macromol.* **2014**, *71*, 94.
[19] M. Buchweitz, J. Brauch, R. Carle, D. Kammerer, *Food Res. Int.* **2013**, *51*, 274.
[20] A. Olad, F. F. Azhar, *Ceram. Int.* **2014**, *40*, 10061.
[21] H. Hoffmann, M. Reger, *Adv. Colloid Interface Sci.* **2014**, *205*, 94.
[22] V. Sovilj, J. Milanović, L. Petrović, *Food Hydrocolloids* **2013**, *32*, 20.
[23] H. Chhabra, P. Gupta, P. J. Verma, S. Jadhav, J. R. Bellare, *Mater. Sci. Eng., C* **2014**, *37*, 184.
[24] B. H. Lee, N. Lum, L. Y. Seow, P. Q. Lim, L. P. Tan, *Materials* **2016**, *9*, 797.
[25] D. I. Hitchcock, *J. Gen. Physiol.* **1931**, *14*, 685.
[26] A. J. Kuijpers, G. H. Engbers, J. Krijgsveld, S. A. Zaat, J. Dankert, J. Feijen, *J. Biomater. Sci., Polym. Ed.* **2000**, *11*, 225.
[27] V. B. Djagny, Z. Wang, S. Xu, *Crit. Rev. Food Sci. Nutr.* **2001**, *41*, 481.
[28] H. G. Schwick, K. Heide, *Bibl. Haematol.* **1969**, *33*, 111.
[29] S. Young, M. Wong, Y. Tabata, A. G. Mikos, *J. Controlled Release* **2005**, *109*, 256.
[30] Y. Ikada, Y. Tabata, *Adv. Drug Delivery Rev.* **1998**, *31*, 287.
[31] H. Fan, C. Zhang, J. Li, L. Bi, L. Qin, H. Wu, Y. Hu, *Biomacromolecules* **2008**, *9*, 927.
[32] Y. Zhang, H. Ouyang, C. T. Lim, S. Ramakrishna, Z. M. Huang, *J. Biomed. Mater. Res.* **2005**, *72B*, 156.
[33] J. Vandervoort, A. Ludwig, *Eur. J. Pharm. Biopharm.* **2004**, *57*, 251.
[34] S. A. Khan, M. Schneider, *Macromol. Biosci.* **2014**, *14*, 1627.
[35] R. C. Oppenheim, *Int. J. Pharm.* **1981**, *8*, 217.
[36] E. J. Lee, S. A. Khan, J. K. Park, K. H. Lim, *Bioprocess Biosyst. Eng.* **2012**, *35*, 297.
[37] G. Kaul, M. Amiji, *Pharm. Res.* **2005**, *22*, 951.
[38] Y. W. Won, Y. H. Kim, *J. Controlled Release* **2008**, *127*, 154.
[39] N. T. Qazvini, S. Zinatloo, *J. Mater. Sci.: Mater. Med.* **2011**, *22*, 63.
[40] S. Fuchs, M. Kutscher, T. Hertel, G. Winter, M. Pietzsch, C. Coester, *J. Microencapsulation* **2010**, *27*, 747.
[41] E. Gevaert, T. Billiet, H. Declercq, P. Dubruel, R. Cornelissen, *Macromol. Biosci.* **2014**, *14*, 419.
[42] S. A. Khan, M. Schneider, *Macromol. Biosci.* **2013**, *13*, 455.
[43] S. A. Galindo-Rodriguez, F. Puel, S. Briancon, E. Allemann, E. Doelker, H. Fessi, *Eur. J. Pharm. Sci.* **2005**, *25*, 357.
[44] B. V. K. Naidu, A. T. Paulson, *J. Appl. Polym. Sci.* **2011**, *121*, 3495.
[45] J. K. Li, N. Wang, X. S. Wu, *J. Pharm. Sci.* **1997**, *86*, 891.
[46] I. Ofner, ClydeM. , W. A. Bubnis, *Pharm. Res.* **1996**, *13*, 1821.
[47] W. A. Bubnis, C. M. Ofner, 3rd, *Anal. Biochem.* **1992**, *207*, 129.
[48] R. Hafidz, C. Yaakob, I. Amin, A. Noorfaizan, *Int. Food Res. J.* **2011**, *18*, 813.
[49] S. Hermanto, L. O. Sumarlin, W. Fatimah, *J. Food Pharm. Sci.* **2013**, *1*, 68.
[50] C. A. Fitch, G. Platzer, M. Okon, B. E. Garcia-Moreno, L. P. McIntosh, *Protein Sci.* **2015**, *24*, 752.
[51] A.-V. Weiss, T. Fischer, J. Iturri, R. Benitez, J. L. Toca-Herrera, M. Schneider, *Colloids Surf., B* **2019**, *175*, 713.
[52] X. Zhai, *Ph.D. Thesis*, Freie Universität Berlin **2014**.
[53] D. C. Phillips, *Proc. Natl. Acad. Sci. U. S. A.* **1967**, *57*, 483.
[54] T. Masuda, N. Ide, N. Kitabatake, *Chem. Senses* **2005**, *30*, 667.
[55] R. Singh, J. W. Lillard, Jr., *Exp. Mol. Pathol.* **2009**, *86*, 215.
[56] Y. H. Liao, M. B. Brown, G. P. Martin, *J. Pharm. Pharmacol.* **2001**, *53*, 549.